

**Analytical solution of space probability distributions of particles in a one-dimensional ring**Haihong Li,<sup>1</sup> Zhoujian Cao,<sup>1</sup> and Gang Hu<sup>2,1,3,\*</sup><sup>1</sup>*Department of Physics, Beijing Normal University, Beijing 100875, China*<sup>2</sup>*Center of Advanced Science and Technology, Beijing Normal University, Beijing 100875, China*<sup>3</sup>*The Key Laboratory of Beam Technology and Material Modification of the Ministry of Education, Beijing Normal University, Beijing 100875, China*

(Received 7 October 2002; published 11 April 2003)

Spatial probability distributions of a few particles having nonidentical masses in one-dimensional space with both periodic and fixed boundary conditions are analytically computed in statistical equilibrium states, and explicit solutions of the probability distributions are obtained. Some nontrivial interesting features of the probability distributions are predicted and fully confirmed by numerical simulations. The realization of a microcanonical equilibrium state of the system is justified by the agreement between the theoretical predictions and numerical observations.

DOI: 10.1103/PhysRevE.67.041102

PACS number(s): 05.20.Jj, 05.70.Fh, 61.20.Gy

**I. INTRODUCTION**

In recent decades the problem of equilibrium states of few-body systems has attracted much attention [1–11]. The interest in this problem rests on the fundamental significance of the link between mechanics and statistical physics. It is now clear that statistical behavior such as microcanonical distributions and associated quantities like temperature, entropy, free energy, and so on can be observed in chaotic low-dimensional mechanical systems. This is in contrast to the long-existing understanding that these statistical quantities can be defined only in macroscopic systems consisting of huge numbers of microscopic subsystems.

In few-body systems, some analytical computations of statistical quantities directly from the corresponding Hamiltonians become possible. In particular, probability distributions of particles can be explicitly calculated in some simple cases. These exact solutions are important and instructive; they can be used for confirming the ergodic theory by comparing with numerical simulations, and also as a starting point for further perturbation treatments. Note that in statistics very few nontrivial analytical solutions are available even for few-body systems. So far, most explicit solutions have been obtained for moment (or, say, velocity) probability distributions, and many fewer analytical results for space probability distributions are known because of some difficulties of space configuration computation. In Refs. [11] and [12], an explicit solution for the two-particle system in a two-dimensional rectangle is obtained, and this exact solution can well explain the interesting van der Waals effect and the associated liquid-solid-like transition in a two-body system [10,12]. Thus, it is significant to find some other nontrivial exact solutions in few-body statistics.

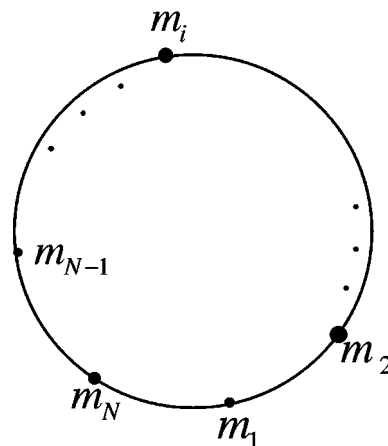
One of the simplest systems showing chaos and a microcanonical probability distribution on the energy surface is a one-dimensional (1D) many-body system. The typical model can be described as follows.  $N$  particles (dimensionless hard dots) are distributed in a 1D ring; the masses of the

particles may take arbitrary real values which may be different from each other. The Hamiltonian of the system is given by

$$H = \sum_{i=1}^N \frac{p_i^2}{2m_i}, \quad P_i = m_i \dot{x}_i, \quad (1)$$

where  $x_i$  is the space position of the  $i$ th particle in the ring and the length of the ring is  $L$ . Moreover, the particles cannot penetrate through each other, and elastic interactions are defined whenever two dots collide with each other. A schematic figure of the model is shown in Fig. 1.

The statistical behavior of the system Fig. 1 has been investigated in detail [3,13,14]. It is confirmed that this 1D  $N$ -body system can reach a microcanonical probability distribution (i.e., statistical equilibrium) in the long-time average whenever  $N \geq 3$  and the masses of the particles are not all identical. In [3] the equilibrium moment distributions of the particles of Fig. 1 are explicitly given, and these distributions were confirmed by numerical simulations. However, for space distributions only some numerical results are available, and no analytical results have been obtained. An exact solution for both moment and space distributions would certainly be useful for understanding the statistical behavior of

FIG. 1. Schematic figure of an  $N$ -body system in circular space.

\*Author to whom correspondence should be addressed.

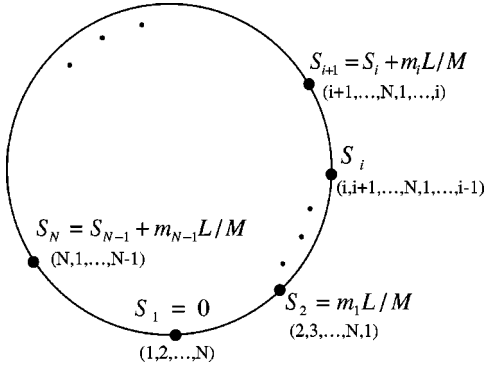


FIG. 2. Distribution of the  $N$  special points  $S_1, \dots, S_N$  given in Eqs. (7), where all particles gather together with certain orderings.

such a typical and important model, and this exact solution may serve as the basis for further analysis of more complicated and realistic systems. The task of this paper is to compute the exact space distribution of the system Fig. 1 and compare the theoretical solution with a numerical simulation.

In Secs. II and III we derive the explicit form of the space probability distribution of a 1D  $N$ -body and nonidentical-mass system. In Sec. IV we set the mass of one particle to infinity, and derive the solution for a hard-ball system. Some interesting results contrary to intuition are obtained. In Sec. V the system statistics is numerically computed, and the numerical results fully agree with the theoretical predictions. Section VI presents a brief discussion and conclusions.

## II. DISTRIBUTIONS OF MOTION RANGES OF VARIOUS PARTICLES

It has been numerically confirmed that the system Fig. 1 can reach statistical equilibrium in the long-time average, i.e., it can reach an equal-probability distribution on the given energy surface [3]. The task in this and the next sections is to explicitly compute the space probability distribution by assuming the microcanonical distribution state. In the present section we first focus on the distributions of motion ranges of various particles.

First, the motion of system (1) is restricted by the total moment conservation law, i.e.,

$$\sum_{i=1}^N m_i \dot{x}_i = 0, \quad (2)$$

which leads to a constraint on the space distribution:

$$\sum_{i=1}^N m_i x_i = \text{const} = 0, \quad (3)$$

where we set the constant to zero without losing any generality.

From ergodicity (which must be valid for statistical equilibrium state) and the constraint (3) we can extract some interesting characteristics of the space distributions of the particles. Because of ergodicity, the following state must be reached during the system evolution:

$$x_1 = x_2 = \dots = x_N = 0. \quad (4)$$

In this state, all the  $N$  particles come together to the same space point  $x=0$ . Since the particles cannot penetrate through each other, the  $N$  particles must follow a necessary order even at the same point; this ordering is assumed to be  $1 \rightarrow 2 \rightarrow 3 \rightarrow \dots \rightarrow N$ , i.e., particle 1 is the leftmost and particle  $N$  is the rightmost. We call the space point  $x=0$  where all the particles come together in the order  $1 \rightarrow 2 \rightarrow 3 \rightarrow \dots \rightarrow N$  the  $S_1$  point (i.e., particle 1 is the leftmost). Now we have  $S_1 = 0$ .

Because of the constraint (3) and nonpenetrability of the particles, particle 1 cannot move right (cannot move anticlockwise from  $x=0$ ), and it has the right boundary of motion at  $x=0$ . However, particle 1 can move left from  $x=0$  (can move clockwise from  $x=0$ ); the left boundary of particle 1 is also defined by the constraint (3) as

$$m_1(L-x) = \sum_{i=2}^N m_i x_i, \quad (5)$$

$$x = S_2 = m_1 L / M, M = \sum_{i=1}^N m_i.$$

At  $S_2$  all particles come together again. However, the ordering is now changed to  $2 \rightarrow 3 \rightarrow \dots \rightarrow N \rightarrow 1$ , where the leftmost particle is particle 2. Thus we call this accumulation point  $S_2$ .

We define  $\widehat{S_i S_j}$  as an arc, which links  $S_i$  to  $S_j$  along the anticlockwise path in the ring of Fig. 1. Thus, particle 1 can never enter the region  $\widehat{S_1 S_2}$ , but it can move in the whole region of  $\widehat{S_2 S_1}$ .  $S_1$  and  $S_2$  are two boundaries restricting the motion of particle 1.

Again particle 2 cannot move anticlockwise from  $S_2$  but it can move left from  $S_2$ , and the leftmost point of particle 2 is also defined by Eq. (3) as

$$m_2(L+x+S_2) = \sum_{i \neq 2}^N m_i(x_i - S_2), \quad (6)$$

$$x = S_3 = S_2 + m_2 L / M.$$

Now all particles can come together to the same point  $S_3$ , at which particle 3 is the leftmost, and the ordering reads  $3 \rightarrow 4 \rightarrow \dots \rightarrow N \rightarrow 1 \rightarrow 2$ . The region  $\widehat{S_2 S_3}$  is forbidden for particle 2 while the whole area  $\widehat{S_3 S_2}$  is reachable for this particle.

The above discussion can be extended to all particles. Based on the ergodicity of the system, nonpenetrability of the particles, and the total moment conservation law of Eq. (3), we can reach some interesting and general conclusions summarized as follows.

(1) For an  $N$ -particle system there are  $N$  particular space points in the ring of Fig. 1, which can be defined as

$$S_1 = 0, \quad S_{i+1} = S_i + m_i L / M, \quad i = 1, 2, \dots, N-1. \quad (7)$$

The distributions of  $S_i$  are schematically drawn in Fig. 2. At these space points, all the particles may assemble, but with different orderings at different points. At point  $S_i$ , the particle ordering reads

$$i \rightarrow i+1 \rightarrow \dots \rightarrow N \rightarrow 1 \rightarrow 2 \rightarrow \dots \rightarrow i-1 \quad (8)$$

(while  $i=1$ , the ordering is  $1 \rightarrow 2 \rightarrow \dots \rightarrow N$ ).

(2) The above space points play important roles in restricting the regions of motions of various particles. For instance, the region  $S_i \widehat{S}_{i+1}$  is forbidden for particle  $i$ . Thus, a nonzero space probability distribution of particle  $i$  exists only in the region of  $\widehat{S}_{i+1} S_i$ . The length of the forbidden region of particle  $i$  is proportional to its mass value  $m_i L / M$ .

In [3], numerical results qualitatively revealed some characteristics of (1) and (2); however, no explicit analysis and quantitative measures were available, and the mechanism underlying these features and the existence of the  $N$  accumulation points  $S_i$ , distinguishing the forbidden zones of various particles, were unknown.

### III. SPACE PROBABILITY DISTRIBUTIONS IN THE RING SYSTEM

From the discussion of Sec. II, we know that, as  $N$  ( $N > 3$ ) elastic and nonpenetrable particles, with nonidentical masses, move in a 1D ring, the motion of each particle is restricted if the total moment is scaled to zero. Then the  $i$ th particle has nonzero probability only in the region  $S_{i+1}[S_i$  defined in Eq. (7). In this section we compute the space probability distributions of all particles in their ranges of motion.

Since we accept an equal-probability distribution on the energy surface and the space variables are not included in the energy expression of Eq. (1), the space probability distribution can be analytically computed based on the equal-probability principle for different space configurations under the total moment conservation condition of Eq. (3) and the nonpenetrability restriction.

We deduce the probability distribution of particle  $N$  in the periodic boundary case. Since there is symmetry with respect to the index of the particles, we can get the probability distributions of all other particles directly from that of the particle  $N$  by changing the index. We can set the mass center of the  $N$ -particle system at  $x=0$ .

First we introduce four characters:

$$M_i = \sum_{j=1}^i m_j, \quad M = \sum_{j=1}^N m_j, \quad i = 1, 2, \dots, N-1,$$

$$B_i(x_{i+1}, x_{i+2}, \dots, x_N) = -\frac{\sum_{j=i+1}^N m_j x_j}{M_i}, \quad i = 2, 3, \dots, N-1,$$

$$E_i(x_{i+1}, x_{i+2}, \dots, x_N) = \frac{\sum_{j=1}^{i-1} m_j(L-x_N) - \sum_{j=i+1}^N m_j x_j}{m_i},$$

$$i = 2, 3, \dots, N-1,$$

$$C_i^{(j)}(x_{i+1}, x_{i+2}, \dots, x_N) = \frac{\sum_{k=1}^{i-j-1} m_k(L-x_N) - \sum_{k=i+1}^N m_k x_k}{\sum_{k=i-j}^i m_k},$$

$$i = 3, 4, \dots, N-1, j = 1, 2, \dots, i-2.$$

When  $j=0$  we have  $E_i = C_i^{(0)}$ ,  $B_i = C_i^{(i-1)}$ .

If we fix  $x_N, x_{N-1}, \dots, x_{i+1}$ , the range of  $x_i$  is  $B_i < x_i < E_i$ . But when  $x_{i+1} < E_i$ , the range becomes  $B_i < x_i < x_{i+1}$ . In a word,  $B_i < x_i < \min(x_{i+1}, E_i)$ . So the probability for  $x_N$  is

$$\rho(x_N) = \int_{B_{N-1}}^{\min(x_N, E_{N-1})} \int_{B_{N-2}}^{\min(x_{N-1}, E_{N-2})} \dots \times \int_{B_2}^{\min(x_3, E_2)} dx_2 \dots dx_{N-2} dx_{N-1}. \quad (9)$$

Now the problem is when  $E_i < x_{i+1}$  happens. We insert  $C_i^{(j)}$  in this relation and find that, if and only if  $x_{i+1} < C_{i+1}^{(j)}$ ,  $x_i < C_i^{(j-1)}$ . We call  $C_i^{(j)}$  the  $j$ -order middle point of the  $i$ th particle. It is easy to prove that if  $x_i < C_i^{(j+1)}$  then  $x_{i-1} \leq x_i < C_{i-1}^{(j)}$ .

*Claim.* If

$$x_N < S_{i+1}, i = 1, 2, \dots, N-1$$

then

$$C_k^{(j)} > S_{i+1}, k-j > 1+i. \quad (10)$$

*Proof.* We have

$$\begin{aligned} C_k^{(j)} &= \frac{\sum_{l=1}^{k-j-1} m_l(L-x_N) - \sum_{l=k+1}^N m_l x_l}{\sum_{l=k-j}^k m_l} > \frac{\sum_{l=1}^{k-j-1} m_l(L-x_N) - \sum_{l=k+1}^N m_l x_N}{\sum_{l=k-j}^k m_l} = \frac{\sum_{l=1}^{k-j-1} m_l L - \sum_{l=k+1}^N m_l x_N - \sum_{l=1}^{k-j-1} m_l x_N}{\sum_{l=k-j}^k m_l} \\ &> \frac{\sum_{l=1}^{k-j-1} m_l L - \sum_{l=k+1}^N m_l S_{i+1} - \sum_{l=1}^{k-j-1} m_l S_{i+1}}{\sum_{l=k-j}^k m_l} = \frac{\left( \sum_{l=1}^{k-j-1} m_l L - \sum_{l=1}^i m_l L \right) + \sum_{l=k-j}^k m_l S_{i+1}}{\sum_{l=k-j}^k m_l} > S_{i+1}. \end{aligned}$$

According to the above discussion, we can write down the probability distribution as

$$\rho(x_N) = \begin{cases} P_K^N(x_N), & x \in [S_K, S_{K+1}], \quad K = 1, 2, \dots, N-2, \\ P_{N-2}^N(E_{N-1}(x_N)), & x \in [S_{N-1}, S_N], \\ 0, & x \in [S_N, L], \end{cases} \quad (11)$$

with

$$P_1^N(x_N) = A_N \int_{B_{N-1}}^{x_N} \int_{B_{N-2}}^{x_{N-1}} \cdots \int_{B_2}^{x_3} dx_2 \cdots dx_{N-2} dx_{N-1},$$

$$\begin{aligned} P_2^N(x_N) = A_N & \left\{ \int_{B_{N-1}}^{C_{N-1}^{(N-3)}} P_1^{N-1}(x_{N-1}) dx_{N-1} + \int_{C_{N-1}^{(N-3)}}^{x_N} P_1^{N-1}(C_{N-2}^{(N-4)}) dx_{N-1} + \int_{C_{N-1}^{(N-3)}}^{x_N} \int_{C_{N-2}^{(N-4)}}^{x_{N-1}} P_1^{N-2}(C_{N-3}^{(N-5)}) dx_{N-2} dx_{N-1} + \cdots \right. \\ & + \int_{C_{N-1}^{(N-3)}}^{x_N} \int_{C_{N-2}^{(N-4)}}^{x_{N-1}} \int_{C_{N-3}^{(N-5)}}^{x_{N-2}} \cdots \int_{C_j^{(j-2)}}^{x_{j+1}} P_1^j(C_{j-1}^{(j-3)}) dx_j \cdots dx_{N-2} dx_{N-1} + \cdots \\ & \left. + \int_{C_{N-1}^{(N-3)}}^{x_N} \int_{C_{N-2}^{(N-4)}}^{x_{N-1}} \cdots \int_{C_3^{(1)}}^{x_4} \int_{B_2}^{E_2} dx_2 dx_3 \cdots dx_{N-2} dx_{N-1} \right\}, \end{aligned}$$

and generally

$$\begin{aligned} P_K^N(x_N) = A_N & \left\{ \int_{B_{N-1}}^{C_{N-1}^{(N-3)}} P_1^{N-1}(x_{N-1}) dx_{N-1} + \int_{C_{N-1}^{(N-3)}}^{C_{N-1}^{(N-4)}} P_2^{N-1}(x_{N-1}) dx_{N-1} + \cdots + \int_{C_{N-1}^{(N-k)}}^{C_{N-1}^{(N-K-1)}} P_{K-1}^{N-1}(x_{N-1}) dx_{N-1} \right. \\ & + \int_{C_{N-1}^{(N-K-1)}}^{x_N} P_{K-1}^{N-1}(C_{N-2}^{(N-K-2)}) dx_{N-1} + \int_{C_{N-1}^{(N-K-1)}}^{x_N} \int_{C_{N-2}^{(N-K-2)}}^{x_{N-1}} P_{K-1}^{N-2}(C_{N-3}^{(N-K-3)}) dx_{N-2} dx_{N-1} + \cdots \\ & + \int_{C_{N-1}^{(N-K-1)}}^{x_N} \int_{C_{N-2}^{(N-K-2)}}^{x_{N-1}} \cdots \int_{C_j^{(j-K)}}^{x_{j+1}} P_{K-1}^j(C_{j-1}^{(j-K-1)}) dx_j \cdots dx_{N-2} dx_{N-1} + \cdots \\ & \left. + \int_{C_{N-1}^{(N-K-1)}}^{x_N} \int_{C_{N-2}^{(N-K-2)}}^{x_{N-1}} \cdots \int_{C_{K+1}^{(1)}}^{x_{K+2}} P_{K-1}^K(E_{K-1}) dx_{K+1} \cdots dx_{N-2} dx_{N-1} \right\} \\ = A_N & \left\{ \sum_{j=1}^{K-1} \int_{C_{N-1}^{(N-1-j)}}^{C_{N-1}^{(N-2-j)}} P_j^{N-1}(x_{N-1}) dx_{N-1} \right. \\ & \left. + \sum_{j=K+1}^{N-1} \int_{C_{N-1}^{(N-K-1)}}^{x_N} \int_{C_{N-2}^{(N-K-2)}}^{x_{N-1}} \cdots \int_{C_j^{(j-K)}}^{x_{j+1}} P_{K-1}^j(C_{j-1}^{(j-K-1)}) dx_j \cdots dx_{N-1} \right\}, \quad (12) \end{aligned}$$

$$K = 2, 3, \dots, N-2,$$

with  $A_N$  being the normalization coefficient. The analytical expression for the recursion (12) can be used, in principle, for computing the space probability distributions of 1D ring system with any finite numbers of particles.

The general formalism of Eq. (11) can be explicitly specified for small  $N$ . For instance, for  $N=3$  we have

$$\rho(x_3) = A_3 \times \begin{cases} x_3 + \frac{m_3 x_3}{M_2}, & x_3 \in [S_1, S_2], \\ \frac{m_1(L-x_3) - m_3 x_3}{m_2} + \frac{m_3 x_3}{M_2}, & x_3 \in [S_2, S_3], \\ 0, & x_3 \in [S_3, L]. \end{cases} \quad (13)$$

For  $N=4$  we have

$$\rho(x_4) = A_4 \times \begin{cases} \int_{-m_4 x_4 / M_3}^{x_4} \int_{-(m_4 x_4 + m_3 x_3) / M_2}^{x_3} dx_2 dx_3, & x_4 \in [S_1, S_2] \\ \int_{-m_4 x_4 / M_3}^{[m_1(L-x_4) - m_4 x_4] / (m_2 + m_3)} \int_{-(m_4 x_4 + m_3 x_3) / M_2}^{x_3} dx_2 dx_3 \\ \quad + \int_{[m_1(L-x_4) - m_4 x_4] / (m_2 + m_3)}^{x_4} \int_{-[m_4 x_4 + m_3 x_3] / M_2}^{[m_1(L-x_4) - m_4 x_4 - m_3 x_3] / m_2} dx_2 dx_3, & x_4 \in [S_2, S_3] \\ \int_{-m_4 x_4 / M_3}^{[m_1(L-x_4) - m_4 x_4] / (m_2 + m_3)} \int_{-(m_4 x_4 + m_3 x_3) / M_2}^{x_3} dx_2 dx_3 \\ \quad + \int_{[m_1(L-x_4) - m_4 x_4] / (m_2 + m_3)}^{[M_2(L-x_4) - m_4 x_4] / m_3} \int_{-[m_4 x_4 + m_3 x_3] / M_2}^{[m_1(L-x_4) - m_4 x_4 - m_3 x_3] / m_2} dx_2 dx_3, & x_4 \in [S_3, S_4], \\ 0, & x_4 \in [S_4, L]. \end{cases} \quad (14)$$

The equal-spacing rule numerically observed in [3] can be confirmed in Eqs. (13) and (14) and also in Eq. (11) for any finite  $N$  we tested. The long-range periodic ordering can be interpreted as crystallization driven by maximizing the entropy [15,16]. An interesting feature from Eq. (11) is that for an  $N$ -particle system the probability density  $\rho(x)$  has smooth derivatives up to order  $d^{N-3}\rho(x)/dx^{N-3}$ , and  $d^{N-2}\rho(x)/dx^{N-2}$  has discontinuities, while  $d^{N-1}\rho(x)/dx^{N-1}$  diverges. This conclusion can easily be checked for  $N=3$  and 4 systems.

#### IV. SPACE PROBABILITY DISTRIBUTION IN A FIXED BOUNDARY SYSTEM

If one of the  $N$  particles has infinitely large mass, the periodic boundary condition can be changed to a fixed boundary one. In the case of infinite  $m_N$ , Eqs. (7) are reduced to

$$\begin{aligned} S_i &= 0, \quad i = 1, 2, \dots, N-1, \\ S_N &= L. \end{aligned} \quad (15)$$

Now all particles except particle  $N$  can move in the entire space region of length  $L$ , while particle  $N$  is static at  $x=0$ , serving as two hard walls of fixed boundaries.

If we insert Eqs. (15) into Eq. (11) and consider infinite  $m_N$ , the space probability distribution of particle  $i$  can be specified as

$$\begin{aligned} \rho_i(x) &= \frac{(N-1)}{L^{N-1}} C_{N-2}^{i-1} x^{N-i-1} (L-x)^{i-1}, \\ C_N^i &= \frac{N!}{(N-i)!i!}. \end{aligned} \quad (16)$$

It is easy to check that

$$\int_0^L \rho_i(x) dx = 1, \quad i = 1, 2, \dots, N-1, \quad (17)$$

$$n(x) = \sum_{i=1}^{N-1} \rho_i(x) \equiv (N-1)/L.$$

The equal-spacing property found in [3] can be confirmed analytically as

$$\langle x_i \rangle = \int_0^L x_i \rho(x_i) dx = \frac{iL}{N}.$$

An interesting feature of Eqs. (16) is that the spatial probability distributions of all moving particles are totally independent of their masses, in sharp contrast with Eq. (11), where with all masses finite the distributions of particles are apparently mass dependent. In particular, if the mass distribution in the  $(0, L)$  region is asymmetric, the spatial distributions are symmetric. Assume, for instance, that we have  $N-1=3$  moving particles in Fig. 3(a), and  $m_3 \gg m_1$ . Then we may expect that the heavy particle  $m_3$  may move in a more restricted region than the light one  $m_1$ . However, the theoretical predictions of space probability distributions

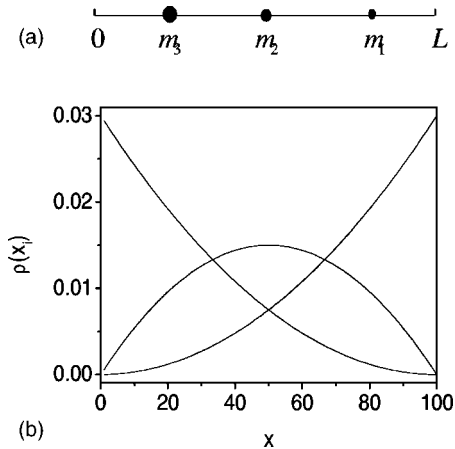


FIG. 3. (a) Three particles moving in a 1D line of length  $L$  with fixed boundary conditions. Mass distribution is asymmetric,  $m_1 = 5$ ,  $m_2 = 2$ ,  $m_3 = 1$ . (b) Symmetric probability distributions of system (a) predicted by Eqs. (16).

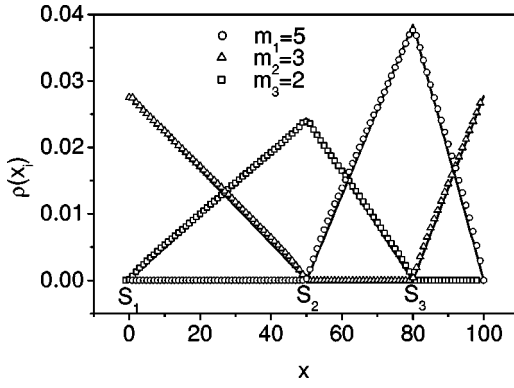


FIG. 4. Space probability distributions of three-particle system in 1D space with periodic boundary conditions.  $m_1=5$ ,  $m_2=3$ , and  $m_3=2$ . At  $S_1=0$ ,  $S_2=20$ , and  $S_3=50$ , the three particles can gather together with the orderings 1,2,3; 2,3,1; and 3,1,2, respectively. The solid line represents the theoretical results Eqs. (13), while circles, triangles, and squares show the numerical observations.

shown in Fig. 3(b) have mirror symmetry between the first and third particles, disregarding the asymmetry of the values of  $m_1$  and  $m_3$ . The mechanism of this feature can be understood as follows: the infinitely large  $m_N$  allows all other remaining  $N-1$  particles to be free from the total momentum conservation law [with  $N$  finite masses, this conservation law plays the central role in determining Eqs. (7) and (11)].

## V. NUMERICAL RESULTS

For confirming the predictions of the space probability distributions in Secs. II–IV, we compute the system statistics numerically. In our simulations the probability distribution of particle  $i$  is calculated by the time average

$$P(x_i, \Delta x_i) = \rho(x_i) \Delta x_i = \Delta \tau_i / T, \quad (18)$$

$$T = \sum_{i=1}^K \Delta \tau_i,$$

where  $\Delta x_i$  is the space step used in measuring  $\rho(x_i)$ . In all our following simulations we take  $\Delta x = L/100$ .  $\Delta \tau_i$  is the time length for particle  $i$  to stay in the space step  $\Delta x_i$  centered at  $x_i$ , and  $T$  is the total time length for our measurement, which is taken to be so large that the system undergoes more than  $10^6$  collisions between the particles.

In Fig. 4 we plot  $\rho(x_i)$  for  $N=3$  and finite masses  $m_1=5$ ,  $m_2=3$ , and  $m_3=2$ . The total energy is an irrelevant quantity and is set to be 297. The solid line represents the theoretical prediction of microcanonical distribution Eq. (13), while all the circles, triangles, and squares show numerical results. It is obvious that numerical simulations confirm the theoretical curves perfectly, indicating that the statistical equilibrium of the equal-probability principle on the energy surface is valid for our simple three-body hard-ball system. In Fig. 5 we do the same as Fig. 4 with  $N=4$  and  $m_1=2$ ,  $m_2=3$ ,  $m_3=4$ , and  $m_4=6$ . In Figs. 6(a) and 6(b) we

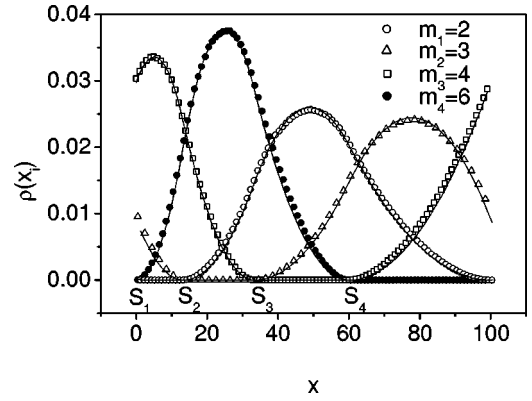


FIG. 5. Same as Fig. 4 with  $N=4$  and  $m_1=2$ ,  $m_2=3$ ,  $m_3=4$ , and  $m_4=6$ . The solid line presents Eqs. (14).

study  $N=5$  and 6, respectively. In all these cases we find complete agreement between the theoretical and numerical results.

In Fig. 7, we take  $N=5$  and let  $m_5 \rightarrow \infty$ . Thus, we consider a four-particle system with fixed elastic boundary conditions. The solid line gives the theoretical result of Eqs. (16), the circles (squares) plot the simulations for  $m_1=10$  ( $m_1=2$ ),  $m_2=5$  ( $m_2=7$ ),  $m_3=2$  ( $m_3=10$ ), and  $m_4=1$  ( $m_4=50$ ). The same space probability distributions are obtained for the numerical plots of different mass distributions, and all numerical results coincide with the theoretical formula. It is clear that asymmetric mass distributions give identical symmetric probability distribution lines, and the

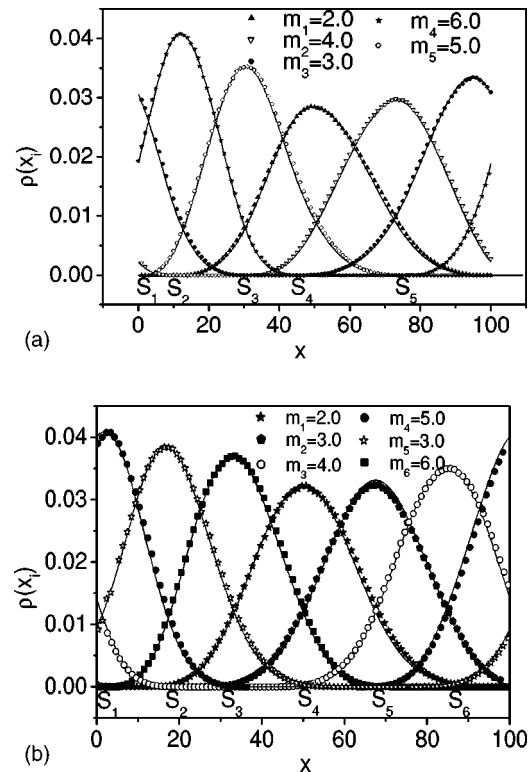


FIG. 6. Same as Fig. 4 with  $N=(a)$  5 and (b) 6. The theoretical predictions are given by Eq. (11).

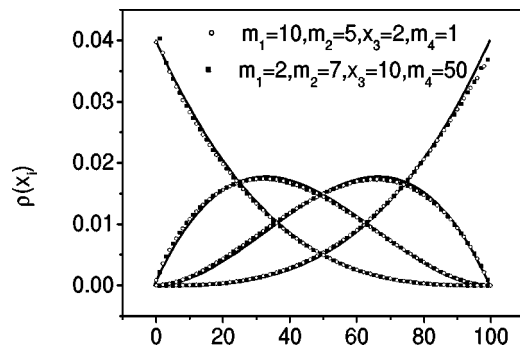


FIG. 7. Same as Fig. 3(b) with  $N=5$ ,  $m_5 \rightarrow \infty$ , i.e., we have fixed boundary conditions with four finite-mass particles. Solid line shows Eqs. (13), and circles and squares are for numerical results for systems with  $m_1=10$ ,  $m_2=5$ ,  $m_3=2$ ,  $m_4=1$  and  $m_1=2$ ,  $m_2=7$ ,  $m_3=10$ ,  $m_4=50$ , respectively.

microcanonical equilibrium distribution of the system for the space variables is convincingly confirmed.

## VI. CONCLUSION

In conclusion, we have analytically calculated the spatial probability distribution of an  $N$ -body hard-ball system in the

1D case for both periodic and fixed boundary conditions. The theoretical solution is significant for the following reasons. First, the 1D  $N$ -body system is among very few important and computable prototypes of few-body systems showing the behavior of statistical physics directly from the first-principles computation of simple mechanical dynamics; thus any nontrivial exact solution with this system is desirable. Second, some features of the solution [such as the existence of  $N$  space points for all-particle gathering  $S_1, \dots, S_N$ ; the regular orderings of the particles at these points; and the structures of the probability distributions of Eqs. (11) and (16); and the discontinuities of some high-order derivatives of the probability distributions  $\rho(x)$ ] were not obviously anticipated before the results came out. Finally, the analytical formulas of Eqs. (11) and (16) for zero-volume-ball ideal systems can be used as a useful perturbation basis in the computations of some nonideal finite-volume-ball systems in multiple-dimensional spaces, such as in a 2D narrow strip or a 3D narrow tube.

## ACKNOWLEDGMENTS

This research was supported by the National Natural Science Foundation of China (10175010) and the Nonlinear Science Project.

- 
- [1] G. Casati, J. Ford, F. Vivaldi, and W. M. Visscher, *Phys. Rev. Lett.* **52**, 1861 (1984).
  - [2] Ya. G. Sinai, *Ergodic Theory with Applications to Dynamical Systems and Statistical Mechanics Systems II* (Springer-Verlag, Berlin, 1989).
  - [3] G. J. Ackland, *Phys. Rev. E* **47**, 3268 (1993).
  - [4] E. Ott, *Chaos in Dynamical Systems* (Cambridge University Press, Cambridge, 1993).
  - [5] Z. Zheng, G. Hu, and J. Zhang, *Phys. Rev. E* **52**, 3440 (1995).
  - [6] Z. Zheng, G. Hu, and J. Zhang, *Phys. Rev. E* **53**, 3246 (1996).
  - [7] S. Sasa and T. S. Komatsu, *Phys. Rev. E* **82**, 912 (1999).
  - [8] S. G. Cox and G. J. Ackland, *Phys. Rev. Lett.* **84**, 2362 (2000).
  - [9] A. Dhar, *Phys. Rev. Lett.* **86**, 3554 (2001).
  - [10] A. Awazu, *Phys. Rev. E* **63**, 032102 (2001).
  - [11] G. Hu, Z. Zheng, L. Yang, and W. Kang, *Phys. Rev. E* **64**, 045102(R) (2001).
  - [12] T. Munakata and G. Hu, *Phys. Rev. E* **65**, 066104 (2002).
  - [13] M. Aizenman, J. L. Lebowitz, and J. Marro, *J. Stat. Phys.* **18**, 179 (1978).
  - [14] J. Masoliver and J. Marro, *J. Stat. Phys.* **31**, 565 (1983).
  - [15] H. N. W. Lekkerkerker, *Physica A* **176**, 1 (1991).
  - [16] P. N. Pusey, W. Van Megan, S. M. Underwood, P. Bartlett, and R. H. Ottewill, *Physica A* **176**, 16 (1991).